

Band structure, Fermi surface, superconductivity, and resistivity of actinium under high pressure

M. Dakshinamoorthy

Department of Physics, Government Arts College, Nandanam, Madras 600035, Tamil Nadu, India

K. Iyakutti

Department of Nuclear Physics, University of Madras, Guindy Campus, Madras 600025, Tamil Nadu, India

(Received 20 March 1984)

The electronic band structures of fcc actinium (Ac) have been calculated for a wide range of pressures by reducing the unit-cell volume from $1.0V_0$ to $0.5V_0$ with use of the relativistic augmented-plane-wave method. The density of states and Fermi-surface cross sections corresponding to various volumes are obtained. Calculations for the band-structure-related quantities such as electron-phonon mass enhancement factor λ , superconducting transition temperature T_c , and resistivity ρ corresponding to different volumes are performed. It is seen that T_c increases with pressure, i.e., with decreasing volume. A new empirical relation for the volume dependence of T_c is proposed and its validity is checked using the T_c values obtained from the above band-structure results. The resistivity ρ first increases with increasing pressure (i.e., with decreasing volume) and then decreases for higher pressures (i.e., for smaller volumes).

I. INTRODUCTION

The actinide metals and their compounds exhibit a wide variety of not well understood, but interesting and unusual phenomena. They have become a subject of great theoretical interest.¹⁻⁵ Until recently little was known about the band structure of the actinide metals with which to interpret their observed electric, magnetic, and optical properties. Ac, the first element in the actinides, has no $5f$ electrons. Here we report the first band-structure calculations of fcc Ac for a wide range of volume from $V=1.0V_0$ to $V=0.5V_0$, V_0 being the volume of the unit cell at normal pressure, thus simulating the high-pressure condition. Earlier, Gupta and Loucks⁶ used the band-structure results of fcc thorium (Th) and invoked the rigid band approximation to obtain the band-structure results of fcc Ac at normal pressure. We⁷ have reported the first full-fledged band-structure calculation of fcc Ac at normal pressure using the relativistic augmented plane-wave (RAPW) method with proper crystal potential, which includes both exchange and correlation via Overhauser's equation.⁸ Nonrelativistic energy band calculations by Kmetto and Hill⁹ and relativistic calculations by Freeman and Koelling^{10,11} have given good evidence that the $5f$ electrons are behaving quite differently in the actinides than the $4f$ electrons in the lanthanides. The continued efforts by Freeman and Koelling¹ have given a clear indication of metallic $5f$ -electron behavior for the actinides at normal pressure. Later Johansson *et al.*¹¹ discussed some aspects of the electronic structure of the actinide metals, both at ambient condition and under pressure. None of the above calculations give any details regarding the band structure, Fermi surface, density of states, and other band-structure related quantities, such as electronic specific heat γ , superconducting transition temperature T_c , and resistivity ρ of Ac under high pressure. So the present calculation is aimed at a detailed investigation of

the band structure, Fermi surface, density of states, and the related physical quantities of Ac under high pressure.

Ac is a heavy element with $Z=89$ and its free-atom configuration is $6d^{17}s^2$. The lattice constant of Ac at normal pressure is 5.331 \AA .¹² In Sec. II, we briefly outline our calculational method. Section III contains the results and discussions on band structure, density of states, and Fermi surface. Section IV deals with the calculations of λ and T_c . In Sec. V, we give the volume dependence of T_c and a simple new empirical relation. Section VI deals with the calculation of resistivity. Finally, in Sec. VII, we give the conclusion.

II. CONSTRUCTION OF CRYSTAL POTENTIAL AND THE METHOD

The crystal muffin-tin potential was constructed using the charge density obtained from the relativistic self-consistent calculations of Liberman¹³ for the free-atom configuration $6d^{17}s^2$. Detailed description of the construction of the muffin-tin potential including exchange and correlation can be found elsewhere.^{14,15} The following expression of Overhauser⁸ for exchange and correlation of the potential is used in computing the muffin-tin potential in atomic units:

$$V_{\text{OH}}^{\text{exc}}(r) = -2.07[\rho(r)]^{-0.3} \quad (1)$$

Using the lattice constant at normal pressure, the lattice constants at different volumes $V=0.9V_0$ to $0.5V_0$ were calculated. For Ac, the lattice constants are not available corresponding to various definite high pressures and also there is no definite relation between pressure and volume in the high pressure region.¹⁶ Hence we have done calculations corresponding to various reduced volumes of the unit cell. Since Ac is a heavy element, the RAPW method was used to compute the band structure. The details of the RAPW method are well known¹⁷ and they are

not repeated here.

The energy bands were calculated using a basis set of 36 reciprocal lattice vectors. The calculations were carried out on a discrete mesh within the first Brillouin zone. The entire zone was partitioned into 2048 cubical volume elements and $E(\vec{k})$ is computed for the \vec{k} point located at the center of each volume element. But because of the symmetry considerations, this involves calculations only for 89 points lying within the irreducible $\frac{1}{48}$ th wedge of the Brillouin zone.

III. RESULTS AND DISCUSSIONS OF THE PRESENT WORK

A. Band structure

The band structures of Ac for the above-mentioned volumes are obtained. But only four band structures corresponding to $V/V_0=1.0, 0.8, 0.7,$ and 0.5 are presented in Figs. 1(a) to 1(d). The band structure is given only

along the symmetry directions $\Gamma-X-W-L-\Gamma-K$. At normal pressure the band structure⁷ is similar to the band structure of Th.^{18,19} The unoccupied $5f$ states never presented a problem in the present case. For Th, $5f$ states got mixed up with the d band and as a result Gupta and Loucks⁶ artificially removed their $5f$ states from the calculations. But in a later calculation for Th by Koelling and Freeman,¹⁸ they could handle the $5f$ states by using the Kohn-Sham Gaspari exchange approximation ($\alpha=\frac{2}{3}$). Here in the present calculation we have used Overhauser's prescription for the exchange and correlation and the unoccupied $5f$ states never interfered with the regular s and d bands. As the volume decreases, the entire band structure is slowly shifted up. (Some of the bands are incompletely drawn due to nonconvergence in the high energy range for some of the \vec{k} points. Since these points are well above the Fermi level, convergence is not tried by increasing the number of RAPW's.) This trend is similar to the high-pressure band structures of lanthanum (La) (Refs. 20–22) and praseodymium (Pr) (Ref. 23).

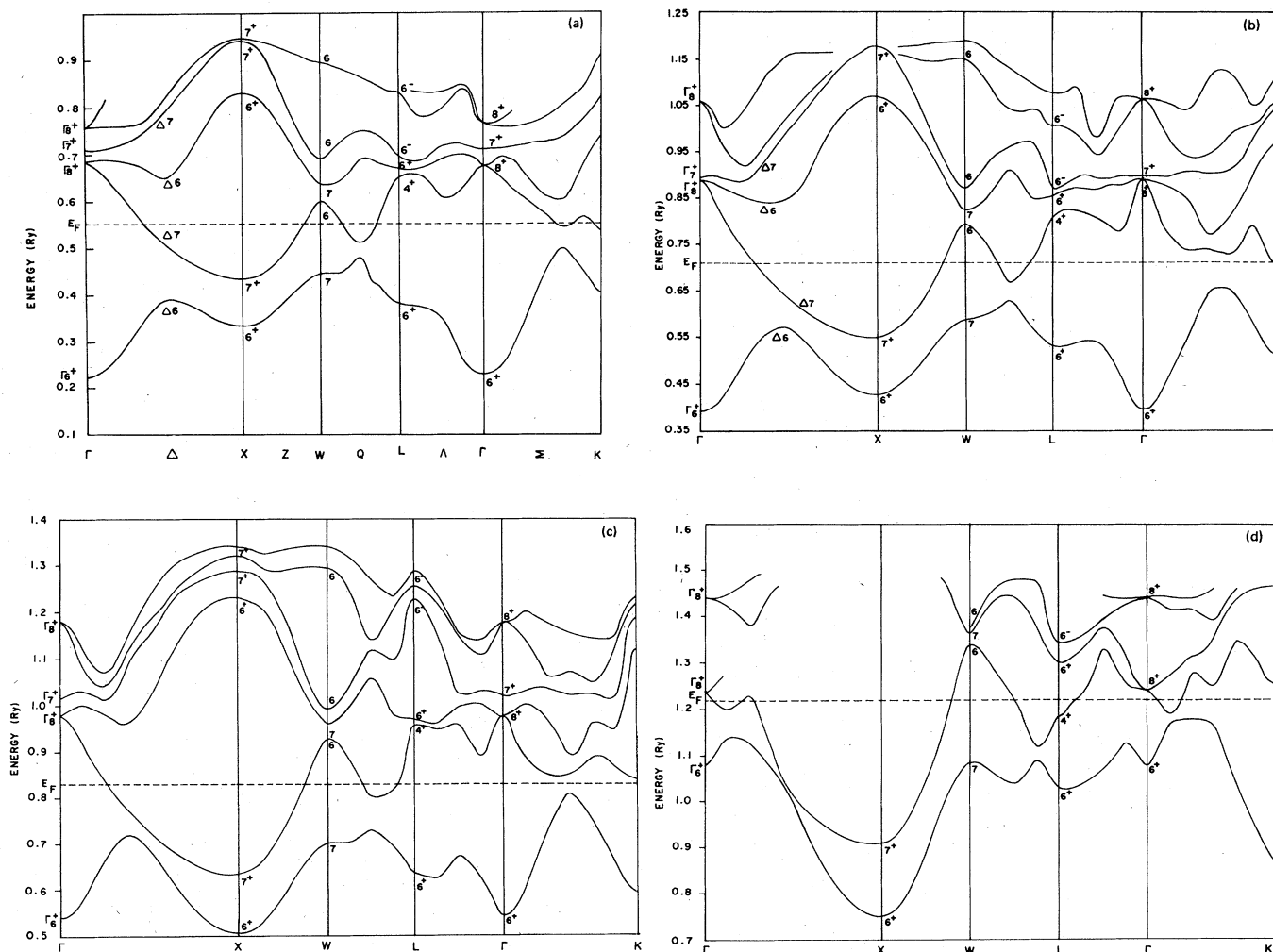


FIG. 1. (a) Band structure of Ac at normal volume V_0 . (b) Band structure of Ac at $V/V_0=0.8$. (c) Band structure of Ac at $V/V_0=0.7$. (d) Band structure of Ac at $V/V_0=0.5$.

The band structure at $V/V_0=0.5$ is entirely different from the band structures at $V/V_0=1.0$ to 0.6 . At the zone center Γ , only the Γ_6^+ , the s derived state lies below Fermi level E_F . At high energies, the eigenvalues are Γ_8^+ , Γ_7^+ , Γ_8^+ . The Γ_8^+ state arises from the atomic d state while Γ_7^+ is due to the f state and they are well above E_F . The $5f$ states are seen to hybridize with the $6d$ and the $7s$ like bands. The overall band structure is that of a transition metal but with f bands which overlap and hybridize to give a more complex structure.²⁴ It is seen that the d and f order remains the same for $V/V_0=1.0$ to 0.5 , but its appearance changes very much at $V/V_0=0.5$. The d and f states are not intertwined at the zone center as observed for La ($4f=0$) by Pickett *et al.*²⁰ and Dakshinamoorthy and Iyakutti.²² It is to be noted that the lowest state at X lies lower than the state Γ_6^+ at Γ from $V/V_0=0.7$ (Fig. 2). The behavior of the eigenvalues at Γ and X under reduction of unit-cell volume is shown in Fig. 3. The occupied d -band region increases under pressure while the occupied s -band region decreases. It is due to the s - d transition under pressure.²¹ It is important to note that along the Γ - K direction the first band never rises above the Fermi level under pressure as observed in La.²⁰⁻²² Further, the dip in the second band below the Fermi level along the Σ direction rises above the Fermi level at $V/V_0=0.8$ but reappears at $V/V_0=0.5$. The dip near the K point below Fermi level disappears as the pressure increases. It is due to the strong hybridization of band structure and the electronic system is strongly coupled to the lattice. The conduction bandwidth at Γ at different unit-cell volumes is listed in Table I. The change in the conduction bandwidth at Γ may be again due to the strong hybridization of band structure with increase of pressure.

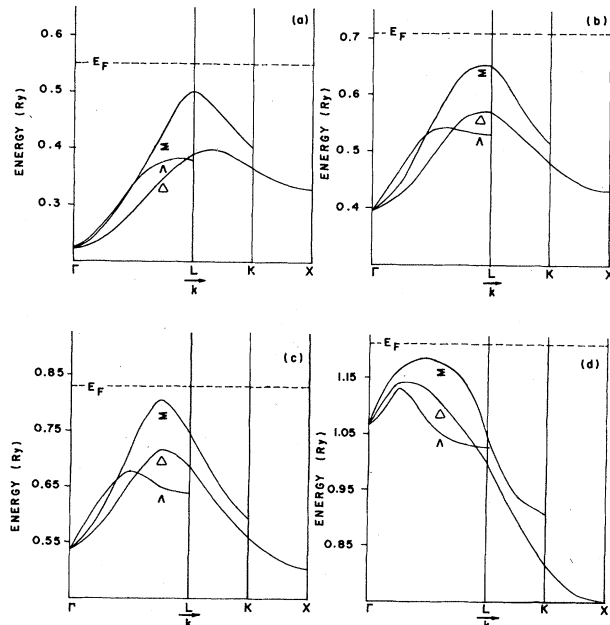


FIG. 2. The Δ , Λ , and Σ branches are shown superposed at four volumes: (a) normal volume V_0 , (b) $V/V_0=0.8$, (c) $V/V_0=0.7$, and (d) $V/V_0=0.5$.

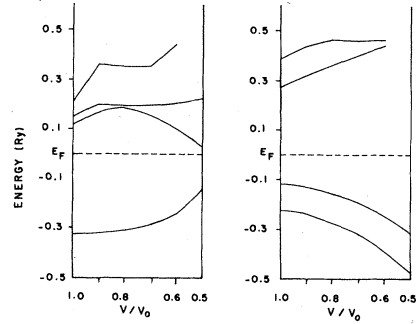


FIG. 3. Behavior of eigenvalues at Γ and X under reduction of unit-cell volume.

B. Density of states

The density of states, $N(E)$, for all the above-mentioned cases has been calculated but the histograms are given only for $V/V_0=1.0, 0.8, 0.7$, and 0.5 [Figs. 4(a) to 4(d)]. The Fermi energies, E_F , corresponding to various pressures are computed and the density of states at E_F , $N(E_F)$ are obtained. It is found that E_F increases with decrease of volume. From the histogram, it is seen that the Fermi levels lie near the peak arising from d -like states in band 2 for $V/V_0=1.0$ to 0.6 [Figs. 4(a) to 4(c)]. But this trend is changed for $V/V_0=0.5$ [Fig. 4(d)]. It is also seen that the huge peaks arising out of f bands are well beyond E_F . The dominant effect of increase of pressure on $N(E)$ is the broadening of bands and it results in the decrease of $N(E)$ in most of the energy regions. The values of E_F and $N(E_F)$ are used in the calculations of γ , λ , T_c , and ρ corresponding to different V/V_0 values. There are no experimental values available for comparison. Corresponding to normal pressure we get the density of states as 11.01 states/atom Ry whereas from the rigid band model of Gupta and Loucks,⁶ this value is 22.6 states/atom Ry.

C. Fermi surface cross sections

We choose to illustrate the Fermi surface of fcc Ac in terms of its cross sections in the three principal planes (100), (110), and (111). The Fermi surface cross sections in these planes for four volumes $V/V_0=1.0, 0.8, 0.7$, and 0.5 are given in Figs. 5–7. At normal pressure, the Fermi surface of Ac is similar to La and Pr.^{20,22,23,25} The entire Fermi surface arises out of band 2. In the figures, the occupied regions are shaded.

In the (100) plane, the area of the electron pocket obtained from the part of the Γ - X and X - W directions, increases with pressure. The electron pocket along the Γ - K direction disappears after normal pressure but reappears close to the zone center Γ for $V/V_0=0.5$. This extends to the Γ - X direction thus enclosing the Γ point [Fig. 5(d)]. However, the electron pocket at the K point at normal pressure disappears as the unit-cell volume is decreased.

In the (110) plane, the size of the electron pockets aris-

ing out of the parts along the $\Gamma-X$, $K-U$, and $X-U$ directions increases as the volume decreases from $V/V_0=1.0$ to 0.8. But afterwards, as the volume decreases further, a neck is developed in the electron pocket creating a hole pocket near the U point [Figs. 6(a)–6(d)]. The area of the hole pocket near the U point increases as the volume decreases. The tiny hole pocket along the $\Gamma-K$ direction at normal pressure disappears for $V/V_0=0.8$. But at $V/V_0=0.5$, the tiny hole pocket is formed again close to zone center Γ , enclosing the Γ

point. The electron pocket along the $L-K$ direction for $V/V_0=0.7$ gets detached from the $L-K$ line and becomes isolated at $V/V_0=0.5$ [Figs. 6(c)–6(d)]. It is seen that the Fermi surface in (110) plane is complicated especially for volumes $V/V_0=0.7$ and 0.5.

In the (111) plane, the area of the electron pocket decreases as the volume decreases from $V/V_0=1.0$ to 0.6 [Figs. 7(a)–7(c)]. It is also to be noted that the lengths of the electron region along the $U-W$ and $W-K$ directions decrease as volume decreases and they vanish at

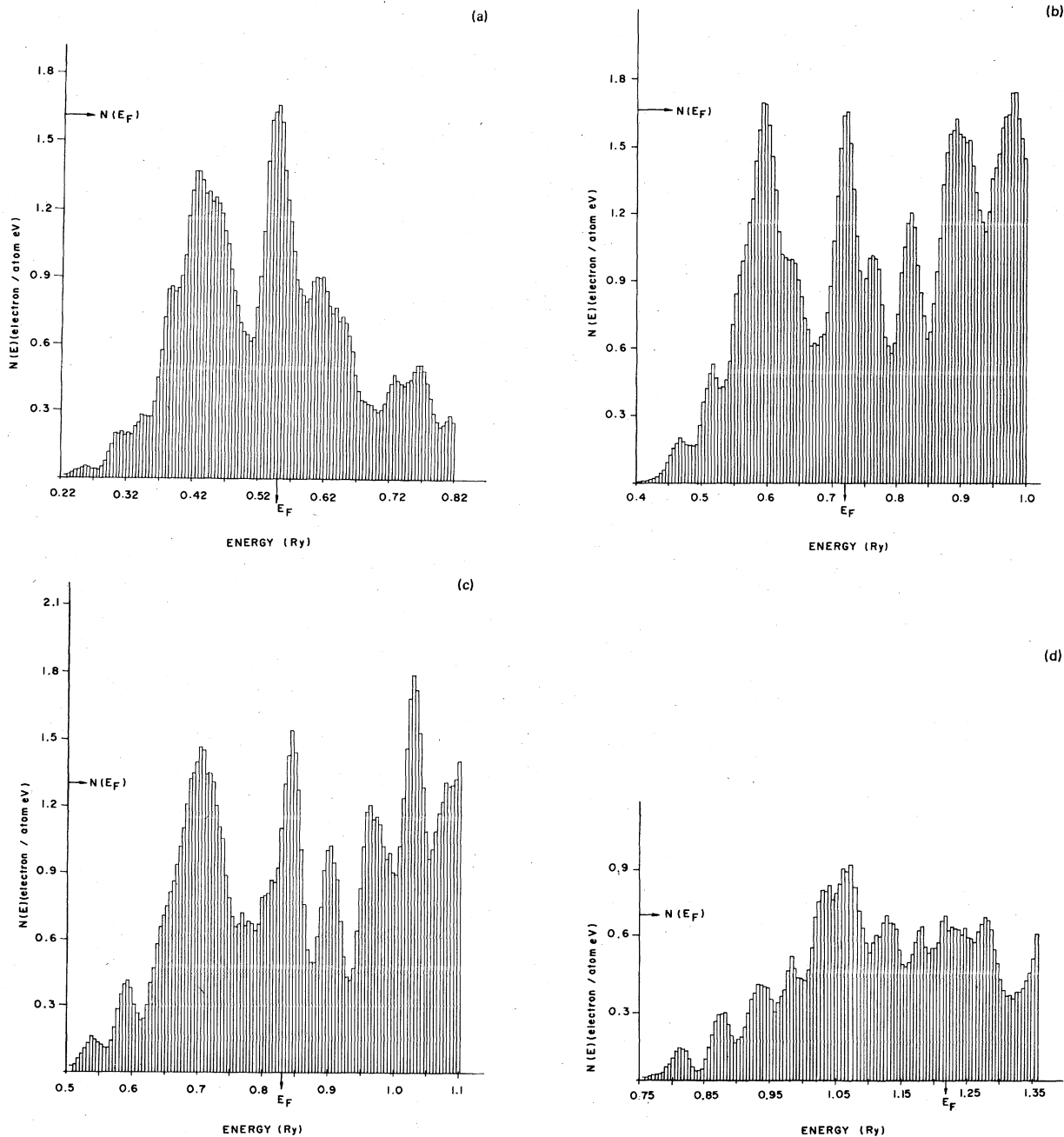


FIG. 4. (a) Density of states histogram of Ac at normal volume V_0 . (b) Density of states histogram of Ac at $V/V_0=0.8$. (c) Density of states histogram of Ac at $V/V_0=0.7$. (d) Density of states histogram of Ac at $V/V_0=0.5$.

$V/V_0=0.7$. The Fermi surface at the (111) plane corresponding to $V/V_0=0.5$ is entirely different in which the electron pocket is formed enclosing the L point [Fig. 7(d)] replacing the hole pocket due to earlier pressures.

IV. THE ELECTRON-PHONON MASS-ENHANCEMENT FACTOR AND THE SUPERCONDUCTING TRANSITION TEMPERATURE

In this section we present the calculations of λ and T_c of fcc Ac. The theory of Gaspari and Gyorffy (GG),²⁶ in conjunction with McMillan's²⁷ formula, is used to calculate T_c . According to GG theory

$$\lambda = \frac{N(E_F)\langle I^2 \rangle}{M\langle \omega^2 \rangle}, \quad (2)$$

where M is the atomic mass, $\langle \omega^2 \rangle^{1/2}$ is an appropriate average phonon frequency, and $\langle I^2 \rangle$ is the square of the electron-phonon matrix element averaged over the E_F . $N(E_F)\langle I^2 \rangle = \eta$ is the electronic stiffness constant.²⁰ For muffin-tin potentials, η (in atomic units) is written as

$$\eta = \frac{E_F}{\pi^2 N(E_F)} \sum_l \frac{2(l+1)}{n_l^{(1)} n_{l+1}^{(1)}} \sin^2(\delta_{l+1} - \delta_l) n_l n_{l+1}, \quad (3)$$

where δ_l is the phase shift of the muffin-tin potential; $n_l^{(1)}$ is the single scatterer l th component of the band-structure density of states. According to GG,

$$n_l^{(1)} = \frac{(2l+1)}{\pi} \left[\delta'_l(E_F) + \frac{1}{2E_F} \chi R_l^2 \times [L_l^2 + L_l - l(l+1) + \chi^2] \right], \quad (4)$$

where $\delta'_l(E_F)$ is the energy derivative of δ_l ; $\chi = \sqrt{E_F} R_0$; R_0 is the APW sphere radius; R_l is the radial wave function at $r = R_0$ and $E = E_F$. It is defined as

$$R_l(r, E) = j_l(r, \sqrt{E}) \cos \delta_l(E) - \eta_l(r, \sqrt{E}) \sin \delta_l(E), \quad (5)$$

where j_l is the spherical Bessel function and η_l is the spherical Neumann function. L_l in Eq. (4) is defined as

TABLE I. The conduction bandwidth at Γ and electronic specific heat coefficients γ of Ac at different volumes.

V/V_0	Conduction bandwidth at Γ (Ry)	γ (10^{-4} cal/mol deg ²)
1.0	0.3295	19.132
0.9	0.3240	18.929
0.8	0.3146	18.783
0.7	0.2931	14.864
0.6	0.2392	9.909
0.5	0.1404	7.961

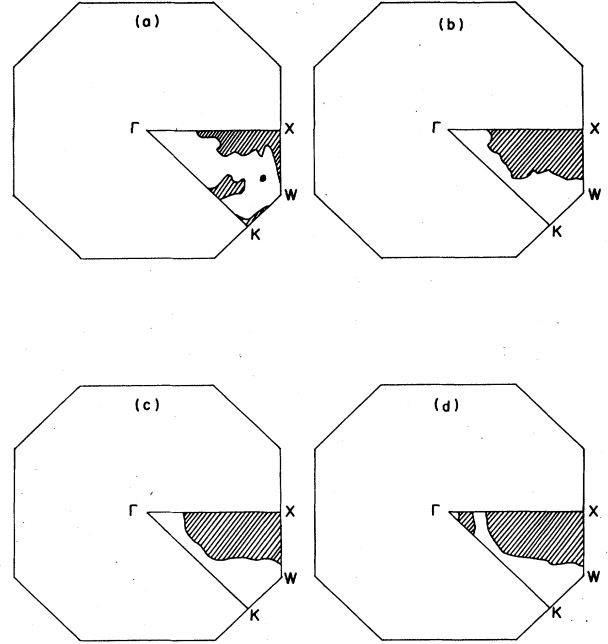


FIG. 5. Fermi surface cross section of Ac in (100) plane. Shaded region indicates electron pocket. (a) Normal volume V_0 , (b) $V/V_0=0.8$, (c) $V/V_0=0.7$, and (d) $V/V_0=0.5$.

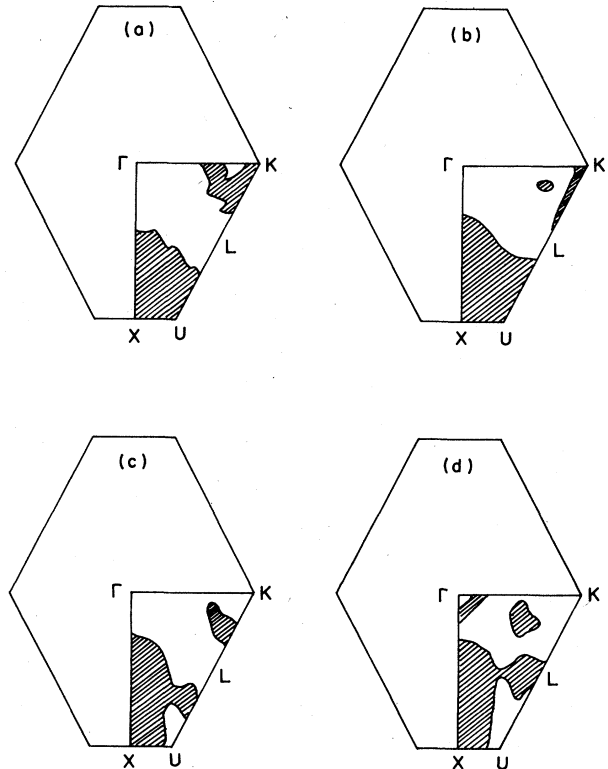


FIG. 6. Fermi surface cross section of Ac in (110) plane. Shaded region indicates electron pocket. (a) Normal volume V_0 , (b) $V/V_0=0.8$, (c) $V/V_0=0.7$, and (d) $V/V_0=0.5$.

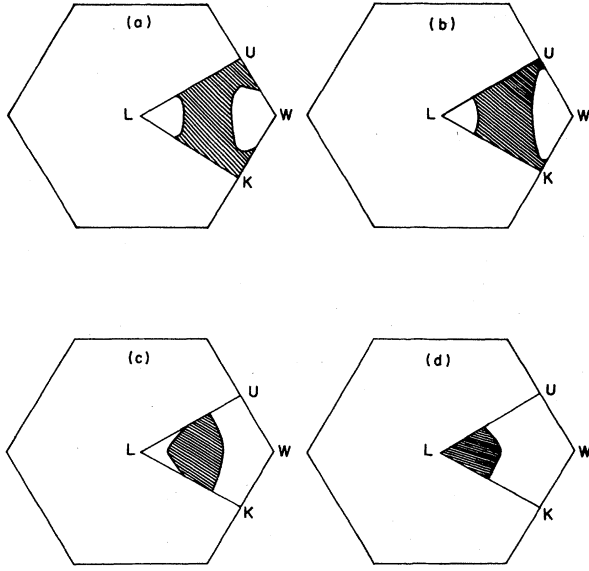


FIG. 7. Fermi surface cross section of Ac in (111) plane. Shaded region indicates electron pocket. (a) Normal volume V_0 , (b) $V/V_0=0.8$, (c) $V/V_0=0.7$, and (d) $V/V_0=0.5$.

$$L_I = R_0 \left[\frac{d}{dr} \ln R_I(r, E_F) \right]_{r=R_0} \quad (6)$$

Following Papaconstantopoulos *et al.*,²⁸ we assume $\langle \omega^2 \rangle = \frac{1}{2} \Theta_D^2$, where Θ_D is the Debye temperature expressed in energy units. The T_c is given by McMillan as

$$T_c = \frac{\Theta_D}{1.45} \exp \left[\frac{-1.04(1+\lambda)}{\lambda - \mu^*(1+0.62\lambda)} \right], \quad (7)$$

where μ^* is the electron-electron interaction parameter. One can also calculate T_c using the relation²⁹

$$T_c = \frac{\omega_{\log}}{1.2} \exp \left[\frac{-1.04(1+\lambda)}{\lambda - \mu^*(1+0.62\lambda)} \right], \quad (8)$$

where ω_{\log} can be approximated³⁰ as $\omega_{\log} = 0.8\omega_g$ and $\omega_g^2 = \frac{1}{2} \Theta_D^2$. Following Asokamani and Iyakutti³¹ we have used the Bennemann and Garland formula for μ^* ,

$$\mu^* = [0.26N(E_F)/2] / [1 + N(E_F)/2]. \quad (9)$$

TABLE II. The electron-phonon mass enhancement factor and superconducting transition temperature T_c of Ac at different volumes.

V/V_0	λ	T_c (K) using Eq. (7)	T_c (K) using Eq. (8)
1.0	1.08724	7.15	4.89
0.9	1.36564	9.52	6.51
0.8	1.70898	11.90	8.14
0.7	2.07810	14.31	9.78
0.6	2.39429	16.32	11.16
0.5	2.63984	17.48	11.95

The T_c values are calculated for various volumes mentioned above using the relations (7) and (8). They are given in Table II. It is seen that T_0 increases with pressure.

V. VOLUME DEPENDENCE OF T_c : A SIMPLE NEW EMPIRICAL RELATION

We have arrived at a new empirical relation for volume dependence of T_c . From the T_c values obtained for various cell volumes as mentioned earlier we wanted to find out whether there exists an empirical relation relating T_c and V . Here we are guided by our earlier work on the pressure dependence of T_c ,³² which was motivated by Wohlfarth's suggestion.³³ We found that the following empirical relation holds good between T_c and V :

$$T_c(V) = T_c(V_0)(1 - V_c/V)^{-1}, \quad (10)$$

where $T_c(V)$ is the superconducting transition temperature corresponding to the volume V and $T_c(V_0)$ corresponds to the normal pressure volume V_0 . The above relation proves its validity by giving a constant V_c value which we call the critical volume. These results are presented in Table III. The critical volume for Ac comes out to be 333.97 a.u. which corresponds to $V/V_0=0.33$. That means when $V/V_0=0.33$ there is singularity in T_c . Here we have to accept that the result arrived at from the empirical relation looks as if it is based on an extrapolation of trends at much larger volumes. Since there are no experimental results available at present, we cannot say anything more regarding this point.

It is interesting to compare this empirical relation [Eq. (10)] with the empirical relation for the pressure dependence of T_c . For the pressure dependence we got³²

$$T_c(P) = T_c(P_0)(1 + P/P_c)^{1/2}, \quad (11)$$

where $T_c(P)$ and $T_c(P_0)$ are the superconducting transition temperatures corresponding to P (in kbar) and normal pressure P_0 , respectively. These two expressions show that the relation between P and V in a solid under pressure is not simple and it is evident from the different exponents occurring in the two relations.

TABLE III. The superconducting transition temperature T_c corresponding to various volumes V and calculation of V_c for Ac.

V (a.u.)	$T_c(V)$ (K) from Eq. (7)	$T_c(V)$ (K) from Eq. (8)	V_c (a.u.) from Eq. (10)
817.816	11.90	8.14	326.55
715.589	14.31	9.78	358.02
613.362	16.32	11.16	344.65
511.135	17.48	11.95	306.65
$T_c(0) = 7.15$ K from Eq. (7)			
$T_c(0) = 4.89$ K from Eq. (8)			
Mean			333.97

TABLE IV. The resistivity ρ of Ac at different volumes.

V/V_0	$(10^{-6} \Omega \text{ cm})$
1.0	227.68
0.9	232.10
0.8	233.00
0.7	222.35
0.6	196.07
0.5	153.94

VI. RESISTIVITY CALCULATIONS

The band-structure results are used to calculate the isothermal resistivity of Ac. Ziman's formula for resistivity involves the structure factor which describes the dynamics of the ions.³⁴ These structure factors are not available to Ac and so we have used the Huang formula³⁵ for resistivity

$$\rho = \frac{2E_F}{3\pi e^2 n^2 \Omega} \sum_l 2(l+1) \sin^2[\delta_l(E_F) - \delta_{l+1}(E_F)], \quad (12)$$

where E_F is the Fermi energy, δ_l is the phase shift of the muffin-tin potential, n is the number of valence electrons per unit volume, and Ω is the volume of the unit cell. The values of ρ corresponding to various V/V_0 are listed in Table IV. It is found that the resistivity increases with pressure initially (low-high pressure region) and then falls on a further increase of pressure (high-high pressure region) (Fig. 8). The resistivity of the actinide metals and metallic compounds behave anomalously compared with those of the rare-earth and transition metals. In the present case, the variation of ρ with pressure is similar to the variation of resistivity with temperature in Pu and PuAl₂.³⁶ It has been shown that the electrical resistivity in some actinide metals, after having a maximum, decreases with increasing temperature due to the s - f dehy-

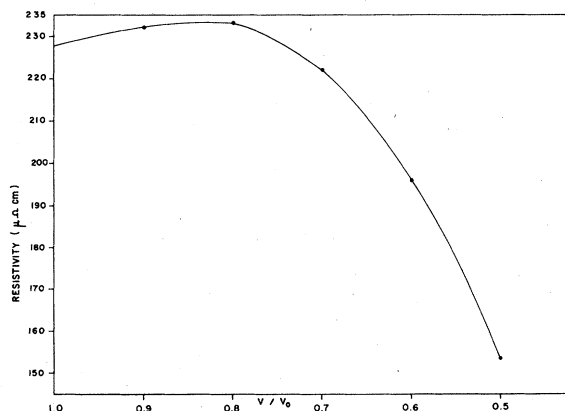


FIG. 8. Variation of resistivity with decrease of volume.

bridization which suppresses the scattering of the s electrons.³⁶ Here, also, in our case the behavior of ρ in Ac as a function of reduced volume may be due to the s - d transition and s - f dehybridization between the unoccupied itinerant $5f$ bands and the $6d$ - $7s$ bands. (It is observed that there is a large drop in resistivity in the volume range $v/v_0=0.6$ to 0.5 . This may be attributed to a phase transition as in the case of Pr.^{37,38})

VII. CONCLUSIONS

From the band structure and density of states histograms, one can see that the f levels are well above the Fermi level. The picture which has emerged for the band structure of this lighter actinide is that of a typical high- Z transition metal with itinerant $5f$ states superposed and strongly hybridized with the $6d$ $7s$ bands.²⁴ The width of the unoccupied (itinerant) f level increases with increase of pressure. But at E_F the effects of the $5f$ bands are small. Corresponding to $V/V_0=0.5$, there is a drastic change in band structure, DOS, and Fermi surface. In the band structure, the bandwidth at Γ attains its minimum value, whereas at X it is maximum and the lowest eigenvalue is at X and not at Γ . In the DOS, the values come down very much because of the wide band spread. The Fermi surface at $V/V_0=0.5$ looks entirely different from the normal pressure Fermi surface. These drastic changes indicate that there may be a structural change in the region $V/V_0=0.6$ to 0.5 . (This prediction is based on the large drop in the resistivity in this volume range, which is supposed to be a signature for any phase transition.^{37,38})

The two sets of T_c values calculated by different relations differ much in their value. In the present case the values of T_c calculated using McMillan's formula seem to be overestimated and the other set of values calculated using the Allan and Dynes²⁹ relation looks reasonable. Anyhow, without any experimental values it is very difficult to judge. But from both the calculations one can see that the T_c value is tending towards a saturation value as the volume is decreased. (The increase in T_c is 2 K by McMillan's formula and 1.38 K by Allen and Dynes formula for a volume decrease from $V/V_0=0.7$ to 0.6 , and for a volume decrease from $V/V_0=0.6$ to 0.5 it is only 1.16 K and 0.79 K, respectively.) Regarding the resistivity calculation, ours is the first calculation to use the Huang formula for resistivity along with the band-structure results. Even though we do not have any experimental value to compare the magnitude of ρ , it looks as though the formula has brought out the pressure dependence (volume dependence) of resistivity.

ACKNOWLEDGMENTS

The authors are thankful to Professor V. Devanathan and Professor T. Nagarajan for their encouragement. Useful discussions with Dr. R. Asokamani are acknowledged with thanks. This work is supported financially through a project by the Department of Atomic Energy, Government of India, India.

- ¹*The Actinides: Electronic Structure and Related Properties*, edited by A. J. Freeman and J. B. Darby, Jr. (Academic, New York, 1974), Vols. I and II.
- ²*Physics of Solids Under High Pressure*, edited by J. S. Schilling and R. N. Shelton (North-Holland, Amsterdam, 1981).
- ³B. Johansson and H. L. Skriver, *J. Magn. Magn. Mater. (Netherlands)* **29**, 217 (1982).
- ⁴H. L. Skriver, B. Johansson, and O. K. Andersen, *Phys. Ser. (Sweden)* **T1**, 25 (1982).
- ⁵M. S. S. Brooks, *J. Phys. F* **13**, 103 (1983).
- ⁶R. P. Gupta and T. L. Loucks, *Phys. Rev. B* **3**, 1834 (1971).
- ⁷K. Iyakutti, M. Dakshinamoorthy, and R. Asokamani, *Solid State Commun.* **40**, 555 (1981).
- ⁸A. W. Overhauser, *Phys. Rev. B* **3**, 1888 (1971).
- ⁹E. A. Kmetto and H. H. Hill, *Plutonium, 70*, edited by W. N. Miner (AIME, New York, 1970), p. 233.
- ¹⁰D. D. Koelling and A. J. Freeman, *Phys. Rev. B* **12**, 5622 (1975).
- ¹¹B. Johansson, H. L. Skriver, and O. K. Andersen, *Physics of Solids Under High Pressure*, Ref. 2, p. 245.
- ¹²R. W. G. Wyckoff, *Crystal Structure* (Interscience, New York, 1963), Vol. I.
- ¹³D. Liberman, *Phys. Rev. B* **2**, 244 (1970).
- ¹⁴R. S. Rao, C. K. Majumdar, B. S. Shastri, and R. P. Singh, *Pramana* **4**, 45 (1975).
- ¹⁵K. Iyakutti, C. K. Majumdar, R. S. Rao, and V. Devanathan, *J. Phys. F* **6**, 1639 (1976).
- ¹⁶S. N. Vaidya and G. C. Kennedy, *J. Phys. Chem. Solids*, **33**, 1377 (1972).
- ¹⁷T. L. Loucks, *Augmented Plane Wave Method* (Benjamin, New York, 1967).
- ¹⁸D. D. Koelling and A. J. Freeman, *Phys. Rev. B* **12**, 5622 (1975).
- ¹⁹K. Iyakutti, R. Asokamani, and V. Devanathan, *J. Phys. F* **7**, 2307 (1977).
- ²⁰W. E. Pickett, A. J. Freeman, and D. D. Koelling, *Phys. Rev. B* **22**, 2695 (1980).
- ²¹A. K. McMahan, H. L. Skriver, and B. Johansson, *Phys. Rev. B* **23**, 5016 (1981).
- ²²M. Dakshinamoorthy and K. Iyakutti, *High Temp. High Pressure* **15**, 645 (1983).
- ²³M. Dakshinamoorthy, K. Iyakutti, S. Sankar, and R. Asokamani, *Z. Phys. B* **55**, 299 (1984).
- ²⁴A. J. Freeman and D. D. Koelling, in *The Actinides: Electronic Structure and Related Properties*, Ref. 1, Vol. I, p. 90.
- ²⁵H. M. Myron and S. H. Liu, *Phys. Rev. B* **1**, 2414 (1970).
- ²⁶G. D. Gaspari and B. L. Gyorffy, *Phys. Rev. Lett.* **29**, 801 (1972).
- ²⁷W. L. McMillan, *Phys. Rev.* **167**, 331 (1968).
- ²⁸D. A. Papaconstantopoulos, L. L. Boyer, B. M. Klein, A. R. Williams, V. L. Moruzzi, and J. F. Janak, *Phys. Rev. B* **15**, 4221 (1979).
- ²⁹P. B. Allen and R. C. Dynes, *Phys. Rev. B* **12**, 905 (1975).
- ³⁰B. M. Klein, W. E. Pickett, D. A. Papaconstantopoulos, and L. L. Boyer, *Phys. Rev. B* **27**, 6721 (1983).
- ³¹R. Asokamani and K. Iyakutti, *J. Phys. F* **10**, 1157 (1980).
- ³²K. Iyakutti and M. Dakshinamoorthy, *J. Phys. F* **13**, L207 (1983).
- ³³E. P. Wohlfarth, *Physics of Solids Under High Pressure*, Ref. 2, pp. 176, 415.
- ³⁴S. N. Kanna, *J. Phys. F* **8**, 1751 (1978).
- ³⁵N. Szabo, *Phys. Rep.* **41C**, 359 (1978).
- ³⁶Yoichi Takaoka and Toru Moriya, *J. Phys. Soc. Jpn.* **52**, 605 (1983).
- ³⁷J. Wittig, *Z. Phys. B* **38**, 11 (1980).
- ³⁸J. Wittig, *Physics of Solids Under High Pressure*, Ref. 2, p. 283.